and Operating Grants Programmes, Imperial Oil of Canada, the Atkinson Foundation, the Connaught Foundation, Erindale College, and the Lash Miller Chemical Laboratories is gratefully appreciated. A.J.L.H. acknowledges the NRCC for a scholarship throughout the duration of her graduate research. We wish also to acknowledge extremely helpful discussions with Professors A. B. P. Lever and H. B. Gray on the subject of the optical spectra of metal tetracarbonyls.

**Registry No.** $Rh(CO)_4$, 28132-77-6; $Ir(CO)_4$, 28132-78-7; $Co(CO)_4$, 58207-38-8; $Pt(CO)_4$, 36344-81-7; $Ni(CO)_4$, 13463-39-3; $Pd(CO)_4$, 36344-80-6; Rh(CO), 66586-41-2; $Rh(CO)_2$, 66454-17-9; $Rh(CO)_3$, 15655-05-7; $Ir(CO)_3$, 70281-27-5; $Ir(CO)_2$, 70281-28-6; Ir(CO), 70281-29-7; $Co(CO)_3$, 58168-83-5; $Co(CO)_2$, 58168-85-7; Co(CO), 58168-84-6.

## References and Notes

(1) D. T. Thompson and R. Whyman in "Transition Metals in Homogeneous Catalysis", G. N. Schrauzer, Ed., Marcel Dekker, New York, 1971.
(2) (a) A. J. Chalk and J. F. Harrod, *Adv. Organomet. Chem.*, **6**, 119 (1968); (b) R. Whyman, *J. Organomet. Chem.*, **81**, 97 (1974).
(3) P. Pino, F. Piacenti, and M. Bianchi, "Organic Synthesis Via Metal Carbonyls", Vol. 2, I. Wender and P. Pino, Eds., Wiley-Interscience, New York, 1977.
(4) (a) E. O. Evans, C. U. Pittman, Jr., R. McMillan, R. T. Beach, and R. Jones, *J. Organomet. Chem.*, **67**, 295 (1974); (b) "Organometallic Polymers", C. E. Carraher, Jr., J. E. Sheats, and C. U. Pittman, Jr., Eds., Academic Press, New York, 1978.
(5) A. C. Yang and C. W. Garland, *J. Chem. Phys.*, **61**, 1504 (1975).
(6) H. Arai and H. Tominaga, *J. Catal.*, **43**, 131 (1976).
(7) H. C. Yao and W. G. Rothschild, *J. Chem. Phys.*, **68**, 4774 (1978).
(8) R. F. Howe, *J. Catal.*, **50**, 196 (1977).
(9) L. Mond, H. Hirtz, and M. D. Cowap, *J. Chem. Soc.*, **97**, 798 (1910).
(10) H. J. Keller and H. Wawersik, *Z. Naturforsch.*, **206**, 938 (1965).
(11) D. R. Bidinosti and N. S. McIntyre, *Chem. Commun.*, 1 (1967).
(12) O. Crichton, M. Poliakoff, A. J. Rest, and J. J. Turner, *J. Chem. Soc., Dalton Trans.*, 1321 (1973).
(13) L. Hanlan, H. Huber, E. P. Kündig, B. R. McGarvey, and G. A. Ozin, *J. Am. Chem. Soc.*, **97**, 7054 (1975).
(14) S. A. Fieldhouse, B. W. Fullam, G. W. Neilson, and M. C. R. Symons, *J. Chem. Soc., Dalton Trans.*, 567 (1974).
(15) M. Elian and R. Hoffmann, *Inorg. Chem.*, **14**, 1058 (1975).
(16) J. K. Burdett, *J. Chem. Soc., Faraday Trans. 2*, **70**, 1599 (1974).
(17) A. J. L. Hanlan and G. A. Ozin, *Ber. Bunsenges. Phys. Chem.*, **82**, 101 (1978).
(18) R. L. DeKock, *Inorg. Chem.*, **10**, 1205 (1971).
(19) E. P. Kündig, M. Moskovits, and G. A. Ozin, *Can. J. Chem.*, **50**, 3587 (1972).
(20) J. H. Darling and J. S. Ogden, *Inorg. Chem.*, **11**, 666 (1972).
(21) P. Kündig, M. Moskovits, and G. A. Ozin, *J. Mol. Struct.*, **14**, 137 (1972).
(22) (a) E. P. Kündig, D. McIntosh, M. Moskovits, and G. A. Ozin, *J. Am. Chem. Soc.*, **95**, 7234 (1973); (b) H. Huber, P. Kündig, M. Moskovits, and G. A. Ozin, *Nature (London), Phys. Sci.*, **235**, 98 (1972).
(23) H. A. Jahn and E. Teller, *Proc. R. Soc. London, Ser. A*, **161**, 220 (1937).
(24) H. Hallam, Ed., "Vibrational Spectra of Trapped Species", Wiley, London, 1973.
(25) D. McIntosh and M. R. Peterson, Vibrational Analysis Programmes, QCPE, 1977.
(26) F. A. Cotton and C. S. Kraihanzel, *J. Am. Chem. Soc.*, **84**, 4432 (1962).
(27) A. J. L. Hanlan, A. B. P. Lever, H. B. Gray, and G. A. Ozin, *Inorg. Chem.*, in press.
(28) (a) I. H. Hillier, M. F. Guest, B. R. Higginson, and D. R. Lloyd, *Mol. Phys.*, **27**, 215 (1975); (b) I. H. Hillier and U. R. Saunders, *ibid.*, **22**, 1025 (1971); (c) J. C. Demuynck, *Chem. Phys. Lett.*, **45**, 74 (1977); (d) J. C. Demuynck and A. Veillard, *Theor. Chim. Acta*, **28**, 241 (1973); (e) D. R. Lloyd and E. W. Schlag, *Inorg. Chem.*, **8**, 2544 (1969).
(29) (a) A. F. Schreiner and T. L. Brown, *J. Am. Chem. Soc.*, **90**, 3366 (1968); (b) H. B. Jansen and P. Ros, *Theor. Chim. Acta*, **34**, 85 (1974); (c) E. J. Baerends and P. Ros, *Mol. Phys.*, **30**, 1735 (1975); (d) R. Osman, C. S. Ewig, and J. R. Van Wazer, *Chem. Phys. Lett.*, **39**, 27 (1976); (e) T. Zeigler, *Acta Chem. Scand., Ser. A*, **28**, 29 (1974); (f) see also ref 28a–c.
(30) N. A. Beach and H. B. Gray, *J. Am. Chem. Soc.*, **90**, 5713 (1968).
(31) A. E. Martell, Ed., "Coordination Chemistry", Vol. 1, Van Nostrand-Reinhold, New York, 1971.
(32) H. Huber, E. P. Kündig, M. Moskovits, and G. A. Ozin, *J. Am. Chem. Soc.*, **95**, 332 (1973).
(33) H. Huber, E. P. Kündig, M. Moskovits, and G. A. Ozin, *Can. J. Chem.*, **50**, 2385 (1972).
(34) E. P. Kündig, M. Moskovits, and G. A. Ozin, *Can. J. Chem.*, **51**, 2710 (1973).
(35) E. P. Kündig, M. Moskovits, and G. A. Ozin, *Can. J. Chem.*, **50**, 3587 (1972).
(36) D. McIntosh and G. A. Ozin, *J. Am. Chem. Soc.*, **98**, 3167 (1976).
(37) L. Malatesta, G. Caglio, and M. Angoletta, *Chem. Commun.*, 532 (1970).
(38) N. N. Kautaradze and N. P. Sokolova, *Dokl. Akad. Nauk SSSR*, **168**, 140 (1966).
(39) C. R. Guerra and J. H. Schulman, *Surf. Sci.*, **7**, 229 (1967).
(40) (a) P. K. Hansma, W. C. Kaska, and R. M. Laine, *J. Am. Chem. Soc.*, **98**, 6064 (1976); (b) R. M. Laine, 172nd National Meeting of the American Chemical Society, San Francisco, Calif., Sept 1976 (private communication).
(41) C. W. Garland, R. C. Lord, and P. F. Troiano, *J. Phys. Chem.*, **69**, 1188 (1965).
(42) J. F. Harrod, R. W. Roberts, and E. F. Rissman, *J. Phys. Chem.*, **71**, 343 (1967).
(43) F. S. Baker, A. M. Bradshaw, J. Pritchard, and K. W. Sykes, *Surf. Sci.*, **12**, 426 (1968).
(44) H. C. Eckstrom, G. C. Possley, and S. E. Hannum, *J. Chem. Phys.*, **52**, 5435 (1970).
(45) C. E. O'Neill and D. J. C. Yates, *J. Phys. Chem.*, **65**, 901 (1961).
(46) L. Lynds, *Spectrochim. Acta*, **20**, 1369 (1964).
(47) M. Moskovits and G. A. Ozin, *Appl. Spectrosc.* **26**, 481 (1972).

Contribution from Lash Miller Chemical Laboratories and Erindale College, University of Toronto, Toronto, Ontario, Canada

# Bimetal Atom Chemistry. 2. Selective Bimetallic Photoaggregation of Ag and Cr Atoms to Very Small Clusters, $Cr_nAg_m$

GEOFFREY A. OZIN* and WERNER E. KLOTZBÜCHER

*Received August 9, 1978*

Silver and chromium form a binary alloy system of the low-miscibility class. By employment of Ag/Cr atom 10–12 K matrix codepositions, selective atomic excitation, and optical spectroscopy it is demonstrated that very small, naked bimetallic clusters of the form AgCr and $Ag_2Cr$ can be selectively photogenerated and identified in the presence of the parents $Ag_{2,3}$ and $Cr_{2,3}$. Extended Hückel molecular orbital techniques are employed to probe the electronic and bonding properties of these unique bimetallic combinations. The implications of these observations for two electronically disparate metals to the left and right of the transition series to Sinfelt's concepts of alloy and bimetallic cluster catalysis are briefly discussed.

## Introduction

Highly dispersed, supported bimetallic and trimetallic clusters are proving to be extremely effective catalysts in the gas–oil–petroleum industries, particularly for such processes as hydrocracking and naphtha re-forming.[1]

Up to the present time, supported multimetallic samples have usually been prepared by coimpregnation and subsequent reduction of an appropriate combination of metal salts.[2b] Unsupported samples may be prepared by similar metal salt reduction techniques,[2c] evaporation of the pure metals,[2d] and leaching of a bulk alloy to give a selected bimetallic catalyst with a high surface area.[2e] However, a question of central concern in high-dispersion multimetallic catalyst systems, especially for mixtures of salts which display little if any miscibility in the bulk phase, is whether one obtains the metal components as separate particles or rather as "multimetallic

0020-1669/79/1318-2101$01.00/0 

**Table I.** Electronic Spectrum (nm) of Disilver, $Ag_2$, Calculated by Several Molecular Orbital Approximations

| transn type | Baetzold data[b] | nucl data[c] | nucl data + 4p[c] | modified nucl data + 4p[d] | SCF-Xα-SW[16] | gas phase[e] | exptl (Ar, 12 K)[d] |
|---|---|---|---|---|---|---|---|
| $s\sigma_g \rightarrow s\sigma_u$ | 788 | 417 | 448 | 415 | 454 | 434 | 388/406[a] |
| $s\sigma_g \rightarrow p\pi_u$ | 554 | 246 | 248 | 251 | 301 | 265 | 258/262[a] |
| $d\pi_g \rightarrow s\sigma_u$ | 254 | 188 | 191 | 233 | 229 | 248 | 227 |

[a] Thought to be a matrix site splitting. [b] Reference 12. [c] Reference 15. [d] This work. [e] Reference 17.

clusters" in which direct interaction between the individual metal components ensues at the atomic level. Evidence for multimetallic clusters in supported and unsupported catalysts may be obtained from catalysis and adsorption studies as the work of Sinfelt has demonstrated.[2a]

Despite the enormous industrial importance of these multimetallic compositions of matter, very little actual atomic detail is known about such properties as geometry and surface structure, surface composition and site segregation, efficiency and uniformity of coclustering, and the effects of the underlying support.[2f] It is known that these clusters are very small and composed of both metal components for bimetallic and all three metals for trimetallic clusters. Unfortunately, the physical methods which are suitable for characterizing supported multimetallic cluster systems are presently limited to the Mössbauer[2f,3] and extended X-ray absorption fine-structure[4] techniques. Information concerning the composition of the outermost atomic layers of high-dispersion catalysts may be obtained from Auger, photoelectron, and flash-desorption spectroscopy, although all of these methods have limitations concerning the quantitative determination of surface content.[2f]

For the Sinfelt Cu/Ru and Cu/Os bimetallic compositions, for example, which fall under the general class of immiscibles, H and CO uptake and ethane hydrogenolysis experiments indicate that a strong interaction exists between the group 8B and group 1B metals.[5a] The data are consistent with the picture of small patches or clusters of copper on the surface of a crystallite composed essentially of pure ruthenium or osmium. For these particular bimetallic combinations, electron microscopy has recently demonstrated the coexistence of both two-dimensional raft and three-dimensional particle structures on silica supports, bringing into the forefront the question of metal–metal vs. metal–substrate bond strength competition effects.[5b]

In view of the exciting potential of multimetallic cluster systems for improving a variety of heterogeneous reactions which currently operate with unimetallic catalysts, it is obviously most desirable to develop new chemical and physical methods for improving our understanding of multimetallic cluster systems at the atomic level.

It is our contention that a useful insight into the electronic and molecular properties of multimetallic combinations can be obtained in the few-atom region by metal atom cryochemical techniques in combination with a suitable form of spectroscopy. For example, we have recently demonstrated that by simultaneously codepositing Cr and Mo atoms with weakly interacting matrix supports at 10–12 K one can generate small $Cr_nMo_m$ clusters which can be subsequently identified by optical spectroscopy.[6,7] In these experiments diatomic and triatomic clusters were produced either on deposition[6] or after deposition by the recently developed selective cryophotoaggregation technique.[7,8] SCF-Xα-SW and EH calculations were also employed in these studies to assist with spectral assignments, bonding, and electronic-structure characterization.[6] The $Cr_nMo_m$ series of small, naked clusters were genuinely bimetallic in the Sinfelt terminology but related to metallic components which were partially miscible in the bulk phase,[9a] owing to their similar electronic structure and minimal size difference. Nevertheless, the usefulness of the method for studying the interactions between two different metals in very small cluster form was established,[9b] and the way was set for an excursion to the more pertinent general class of immiscible and low-miscibility metallic combinations.

In this particular study we have chosen to investigate the rather discrepant atomic combination silver–chromium, two transition metals which, in the bulk, exhibit fccub and bccub crystal structures, respectively, which are of quite different atomic sizes, and whose phase diagrams demonstrate very low-miscibility properties.[9a] (Here one should remember that metal atoms with more than a 15% size difference are in general immiscible.[9a]) Furthermore, these metals are from opposite sides of the periodic table, with electronic configurations and energy levels distinctly different. From a cryochemical standpoint this is an ideal test combination, as Cr and Ag atoms have been individually investigated by metal concentration, bulk annealing, and photoaggregation matrix techniques. Moreover, the optical spectroscopy of $Cr_{2,3}$[6,7] and $Ag_{2-4}$[8] naked clusters is reasonably well understood.

## Experimental Section

Bimetal atom codeposition techniques for the Ag/Cr system were similar to those described for the Cr/Mo experiments.[6] Silver and chromium (99.99%) were both evaporated from tantalum Knudsen cells with the metal flow quantitatively monitored by a dual quartz-crystal microbalance assembly[6] which was simply a modification of the original single quartz-crystal monitor design.[10,11] Research grade argon (99.995%) was supplied by Matheson of Canada. A Displex closed-cycle helium refrigerator was used to cool a NaCl optical window to 10–12 K, with the temperature being monitored by a thermocouple embedded in a drilled cavity 10 mm from the window center. UV–visible spectra were recorded on a Unicam SP 8000 spectrophotometer in the range 200–700 nm. In photoaggregation experiments the radiation of a 450-W Oriel xenon lamp was focused through a 10-cm water cell onto the entrance slit of a Schoeffel GM 100 grating monochromator with the slit width between 1.0 and 2.5 mm (8.5 and 21 nm half-width).

## Results

$Cr_{2,3}$ and $Ag_{2,3}$ small-cluster systems have formed the subject of extensive experimental and theoretical (EHMO, SCF–Xα–SW) investigation.[6-8,19] Each metal atomic species has a ground-state configuration of the type $d^n s^1$, the d shell being half filled for Cr and filled for Ag. Both metal atomic species can be aggregated in a facile manner by codeposition with inert gases and cryophotoclustering matrix techniques at 10–12 K.[6-8] To achieve instrumental compatibility with our chromium cluster data we have reinvestigated some of the earlier silver cluster work.[8] The results were essentially the same except for some slight frequency shifts (calibration effects, Table I). In line with previous observations, we have been unable to form appreciable amounts of $Ag_2$ or $Ag_3$ upon thermal diffusion of matrix-entrapped Ag atoms and conclude that at least for the embryonic nucleation events a small activation energy is required to promote silver–silver bonding.[8] As before, two different matrix sites were observed for $Ag_2$ in Ar, and the facile photogeneration of $Ag_3$ at 12 K and thermal loss at temperatures exceeding 25 K in Ar mirrored past experiences with the small silver cluster system.[8]

Figures 1 and 2 present the photoaggregation of $Ag/Ag_2/Ar$ and $Cr/Cr_2/Ar$ mixtures, respectively, induced by selective

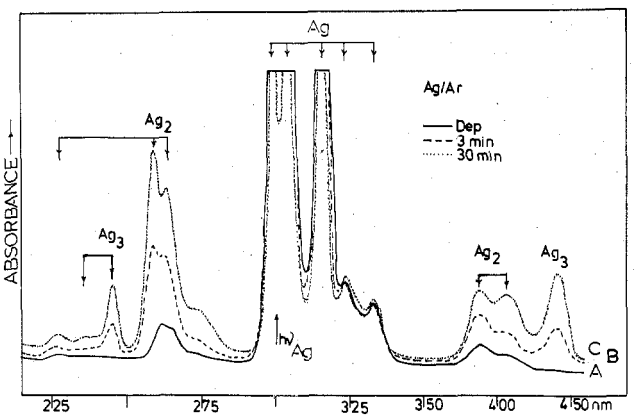


**Figure 1.** Ultraviolet–visible spectrum of (A) a Ag/Ar ≃ 1/1000 mixture deposited at 10–12 K showing Ag and $Ag_2$ clusters followed by (B) 3 min and (C) 30 min of 305-nm Ag atom photoexcitation, showing the photoaggregation of Ag atoms to produce $Ag_2$ and $Ag_3$. (Note scale change between 350 and 400 nm.)

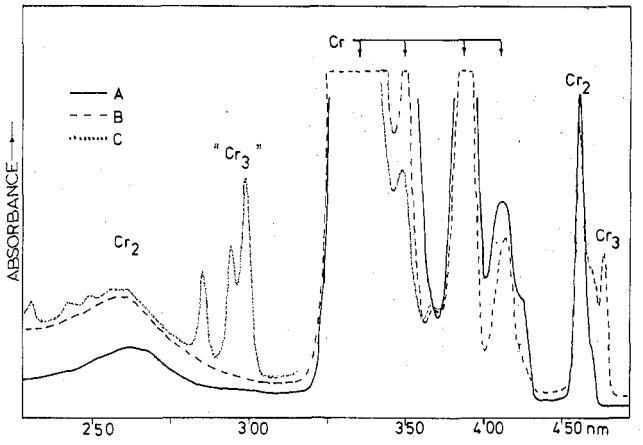


**Figure 2.** Ultraviolet–visible spectrum of (A) a Cr/Ar ≃ 1/1000 mixture deposited at 10–12 K showing Cr and $Cr_2$ clusters and (B) the result of 60 min of 335-nm Cr atom photoexcitation recorded after (C) the metastable $Cr_3$ species had been allowed to decay to zero.

Ag ($4d^{10}5s^1 \rightarrow 4d^{10}5p^1$) and Cr ($3d^54s^1 \rightarrow 3d^44s^14p^1$) narrow-band atomic photoexcitation from a 450-W xenon lamp. In both cases photoaggregation to the $Ag_3$[8] and $Cr_3$[6,7] cluster stages can be readily achieved. One should note here that $M_{1-3}$ mixtures can also be generated in the Ag and Cr systems by metal concentration experiments.[7,8] However, for a number of systems investigated so far, the photoaggregation approach appears to be amenable to a greater degree of control of cluster size.

Of particular importance in the $Cr_n$ and $Ag_n$ small-cluster systems is the optical window in the 275–300 nm region, an energy range which develops special significance in the mixed Ag/Cr/Ar codeposition experiments to be described.

Let us first consider the products of a Cr/Ag/Ar ≃ 1/1/1000 deposition at 10–12 K (Figure 3A), remembering that under comparable Cr/Ar ≃ 1/1000 (Figure 3B) and Ag/Ar ≃ 1/1000 (Figure 3C) conditions only the diatomic cluster stage is achieved. The most striking observation in the Cr/Ag/Ar high-dispersion system is the appearance of a *new* spectral feature centered at 283 nm. Other absorptions which can be associated with a mixed $Cr_nAg_m$ cluster are not observed under these conditions. Clearly, the 283-nm absorption can be given the a priori assignment of AgCr, where other absorptions associated with the heteronuclear diatomic cluster are either (i) too weak to observe under these conditions, (ii) obscured by band overlap with the intense Cr, Ag atomic or $Cr_2$, $Ag_2$ cluster absorptions, or (iii) outside of the range of our instrument capability (200–700 nm). Cr/Ag/Ar concentration experiments confirm that the 283-nm absorption is indeed associated with the first stage of Cr/Ag clustering, that is, AgCr. Only in experiments involving large amounts of material do we actually observe another, very weak absorption at 220 nm which might be associated with AgCr.

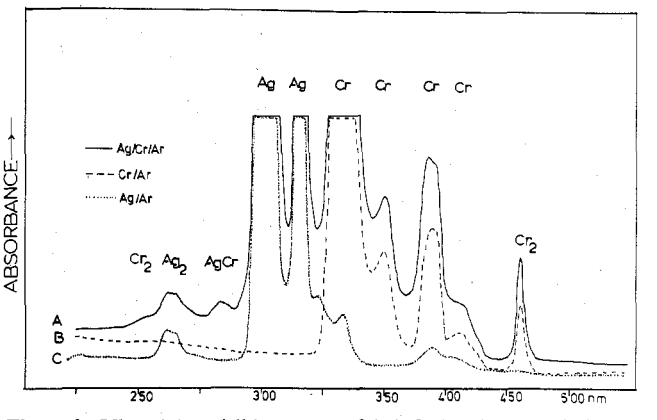


**Figure 3.** Ultraviolet–visible spectra of (A) Cr/Ag/Ar ≃ 1/1/1000, (B) Cr/Ar ≃ 1/100, and (C) Ag/Ar ≃ 1/1000 mixtures deposited at 10–12 K showing the formation of $Cr_2$, $Ag_2$, and AgCr.

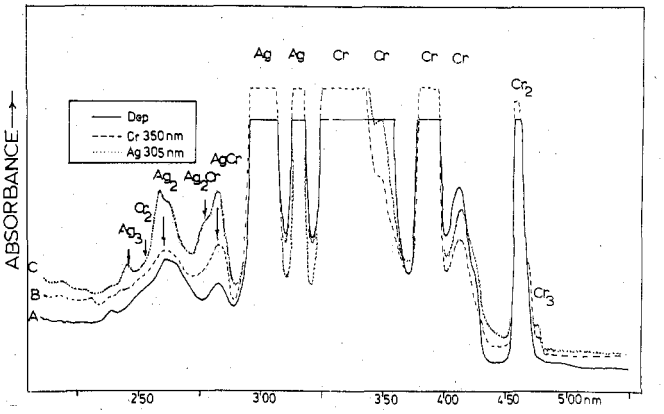


**Figure 4.** Ultraviolet–visible spectrum of a Cr/Ag/Ar ≃ 1/1/1000 mixture (A) upon deposition at 10–12 K showing Cr, Ag, $Cr_2$, $Ag_2$, and AgCr, (B) after Cr atom 350-nm photoexcitation and 30-min relaxation time showing the growth of $Cr_3$ and CrAg, and (C) after Ag atom 305-nm photoexcitation showing the growth of $Ag_2$, $Ag_3$, AgCr, and $Ag_2Cr$.

Let us turn our attention now to the Ag/Cr bimetallic photoaggregation experiments. Figure 4A shows the Ag/Cr/Ar = 1/1/1000 system after deposition at 10–12 K. As in Figure 3, one observes mainly $Cr_2$, $Ag_2$, and AgCr on deposition. Narrow-band Cr ($3d^54s^1 \rightarrow 3d^44s^14p^1$) excitation causes a large decrease in the Cr atomic resonance lines with a concomitant, but much smaller, loss of the Ag atomic resonance lines. Under these conditions both stable and metastable $Cr_3$ species grow in as in the pure Cr/$Cr_2$/Ar system[7] along with a notable increase in the intensity of the AgCr (283-nm) absorption. Figure 4B displays the situation 30 min after irradiation when the metastable $Cr_3$ has decayed to zero. Significantly, the $Ag_2$ absorptions remain essentially unchanged during Cr atom photoexcitation, and the characteristic $Ag_3$ absorptions at 245 and 440 nm do not grow in. All the evidence therefore points in favor of *photoselective bimetallic aggregation upon Cr photomobilization* in the presence of Ag, $Ag_2$, AgCr, and $Cr_2$ species.

Focusing attention on sequential Ag atom photoexcitation as depicted in Figure 4C, one observes a marked decrease in the Ag atomic resonance absorbances with concomitant, but much smaller, loss of the Cr atomic resonance lines. Especially gratifying is the observation of growth of $Ag_2$ and AgCr together with the appearance of $Ag_3$ and a striking *new* spectral

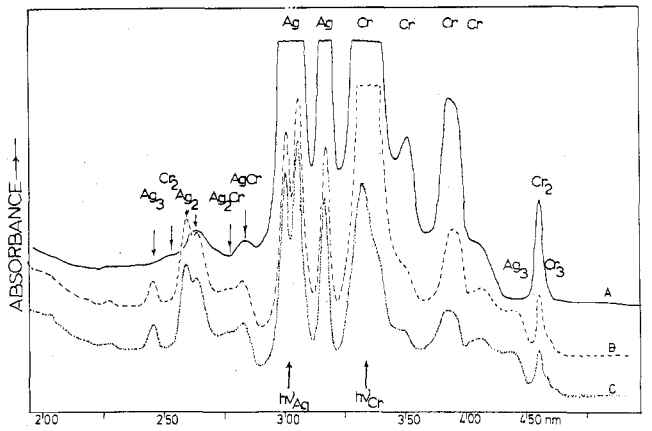


**Figure 5.** Ultraviolet–visible spectrum of a Cr/Ag/Ar ≃ 1/1/1000 mixture (A) upon deposition at 10–12 K showing Cr, Ag, $Cr_2$, $Ag_2$, and AgCr, (B) after Ag atom 305-nm photoexcitation showing the growth of $Ag_2$, $Ag_3$, AgCr, and $Ag_2Cr$, and (C) after Cr atom 350-nm photoexcitation showing the growth of $Cr_3$ and slight growth of AgCr.

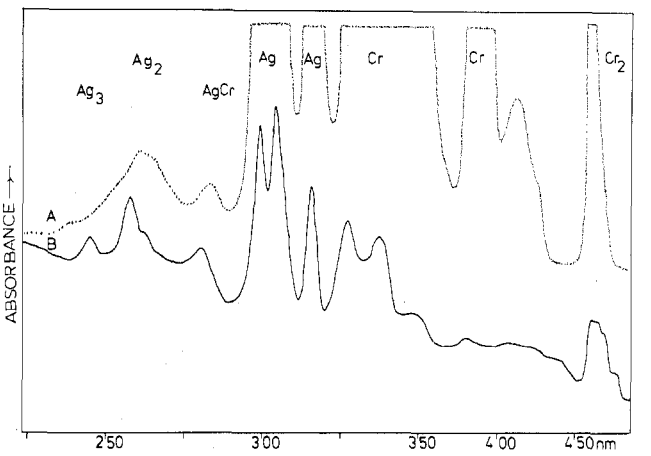


**Figure 6.** Ultraviolet–visible spectrum of (A) a Ag/Cr/Ar = 1/1/1000 mixture deposited at 10–12 K showing Ag, Cr, $Ag_2$, $Cr_2$, and AgCr and (B) the result of 5-min broad-band 250–600-nm irradiation showing "nonselective" photoaggregation of Cr and Ag atoms to $Ag_2$, $Ag_3$, $Cr_3$, AgCr, and higher clusters.

feature at 276 nm as a shoulder on the AgCr absorption at 283 nm. *The results once again emphatically point to the existence of a photoselective bimetallic aggregation phenomenon.* Moreover, from a series of sequential Cr, Ag atomic photoexcitations and Cr/Ag concentration ratio variations, one can conclude that the new absorption at 276 nm is associated with the triatomic mixed-metal cluster $Ag_2Cr$. An absorption unequivocally ascribable to $Cr_2Ag$ has not yet been observed in this system.

Additional experimental support for the concept of photoselectivity in this bimetallic system and the spectral assignment of AgCr and $Ag_2Cr$ stems from a series of experiments similar to those described in Figure 4, except that the aggregation is initiated by Ag rather than Cr photoexcitation. Sequential Ag followed by Cr photoexcitations are illustrated in Figure 5B,C for a Cr/Ag/Ar ≃ 1/1/1000 matrix deposited at 10–12 K. Major Ag and minor Cr atomic resonance line intensity alterations ensue on Ag photoexcitation, and, as expected, $Ag_2$, $Ag_3$, AgCr, and $Ag_2Cr$ grow in (Figure 5B). In line with these spectral appearances, some $Cr_2$ is consumed. The following Cr photoexcitation, depicted in Figure 5C, shows the expected diminution of Cr atomic resonance lines with little accompanying change of Ag atomic absorptions, slight growth of AgCr, appearance of $Cr_3$, and essentially *zero* growth of $Ag_2$ and $Ag_3$. All of these observations are supportive of photoselectivity and consistent with our earlier assignments of AgCr and $Ag_2Cr$.

Further support for our proposals stems from a control experiment in which a Cr/Ag/Ar ≃ 1/1/1000 matrix of the type illustrated in Figure 5A is photolyzed with *broad-band* irradiation covering the region 250–600 nm. Under these conditions both Cr ($3d^54s^1 \rightarrow 3d^44s^14p^1$) and Ag ($3d^{10}4s^1 \rightarrow 3d^{10}4p^1$) electronic transitions are simultaneously excited. The outcome shown in Figure 6 is *nonselective photoaggregation* in which *both* Cr and Ag atomic lines show concurrent major decay accompanied by the growth of $Ag_2$, $Ag_3$, $Cr_3$, AgCr, and some $Ag_2Cr$.

## Extended Hückel Molecular Orbital Calculations on the Diatomic Molecules

Quite a number of researchers have chosen the EHMO approximation as a fast and relatively inexpensive gateway into probing the molecular orbital architecture of diatomic and polyatomic transition-metal clusters.[12,13,25] We have previously reported EHMO results for $Cr_2$, $Mo_2$, and CrMo and compared them to SCF–X$\alpha$–SW calculations on the same molecules.[6] We had found that EHMO calculations spectroscopically parameterized to quantitatively fit the observed electronic transition of $Cr_2$ and $Mo_2$ would not only reproduce bond distances and dissociation energies within the range of experimental error for the homonuclear molecules but also predict reasonably well the electronic transitions, bond length, and dissociation energy of the heteronuclear molecule CrMo.

However, the $Cr_2$, $Mo_2$, and CrMo calculations concerned component atoms which are neighbors in the periodic table, exhibiting similar orbital energies and electronic configurations; close correlation between experiment and theory was therefore not totally unexpected. A more stringent test of the EHMO approach to small-cluster problems would involve the question of two atoms of quite disparate electronic properties. The AgCr molecule provides such a test case. However, it should be emphasized at the outset of this discussion that although the EHMO results of the present $Cr_nAg_m$ study seem entirely reasonable, they must be considered to be highly qualitative in nature, and any attempted quantitative assignment of optical transition energies must be treated with caution.

**Disilver, $Ag_2$.** The $Ag_2$ molecule was investigated extensively by Baetzold[12] several years ago employing EHMO and CNDO methods. In this and other studies, several formulas for calculating the off-diagonal elements were compared. It was found that the Cusach's approximation

$$H_{ij} = \tfrac{1}{2}(2 - S_{ij})(H_{ii} + H_{jj})S_{ij}$$

delivered not unreasonable results. However, it was noted that the Cusach as well as other approximations did not yield minima in the potential energy curves for the first-row transition-metal diatomics.[12] In a later study[14] in our group, this goal was achieved by including 3p orbitals in the basis set.

We have repeated Baetzold's $Ag_2$ calculations and have found that, at the computed equilibrium distance of 3.6 Å, the predicted electronic transitions were quite different from the experimental results (Table I). However, by using VSIOP's from a different source[15] but retaining the 4d, 5s, 5p orbital set, we achieved a much better spectroscopic fit for $Ag_2$ at the minimum-energy geometry of 2.6 Å. To be consistent with our $Cr_2$ calculations, we also included the 4p orbitals in our $Ag_2$ calculations; this did not lead to a major change in the potential minimum, computed at 2.7 Å, nor in the molecular orbital energies. By maintaining the 4d orbital energy constant and lowering the 5s and 5p orbital energies, we obtained a scheme which is in acceptably close agreement with our electronic spectra data (Tables I and II).

In order of increasing energy, the valence orbitals of $Ag_2$ include the six completely filled $\sigma_{g,u}$-, $\pi_{g,u}$-, and $\delta_{g,u}$-bonding

**Table II.** Optical Spectra (nm) Observed for Small $Cr_nAg_m$ Clusters in Solid Argon at 12–15 K

| | | | |
|---|---|---|---|
| $Ag_2$ | 388, 406 | AgCr | 283 |
| | 258, 262 | | 220 |
| | 227 | $Ag_3$ | 440 |
| $Cr_2$ | 460 | | 245 |
| | 263 | $Cr_3$ | 467 |
| | | $Ag_2Cr$ | 276 |

and -antibonding levels of the d band, the occupied $\sigma_g$-bonding and empty $\sigma_u$-antibonding levels of the s band, and the empty $\pi_u$ and $\sigma_g$ virtual levels of the p band. The s and d bands are well separated in $Ag_2$ (they actually overlap in $Cu_2$[16]), which is reflected in the silver–silver bonding as being an almost pure 5s–5s interaction.

Gas-phase $Ag_2$ has been observed by optical spectroscopy and exhibits three major absorption bands at roughly 434, 265, and 248 nm.[17] Recent cryophotochemical cluster experiments[16] have indicated that irradiation into the 400-nm region of matrix-entrapped $Ag_2$ causes photodissociation of $Ag_2$ (as one nonradiative channel), with subsequent Ag and $Ag_3$ formation and isolation. The 400-nm visible absorption was thus assigned to the $s\sigma_g \rightarrow s\sigma_u$ ($A \leftarrow X$) excitation, capable of disrupting the metal–metal bond of matrix-entrapped $Ag_2$, even though the ($A \leftarrow X$) band structure of gaseous $Ag_2$ indicates a weakly bound, excited A state.[17] The higher energy UV bands of $Ag_2$ in solid Ar have been associated with the $s\sigma_g \rightarrow p\pi_u$ ($C \leftarrow X$) and $d\pi_g \rightarrow s\sigma_u$ ($E \leftarrow X$) excitations[17] as listed in Tables I and II. It is interesting to note that *the EHMO data for $Ag_2$ are in very close agreement with a recent SCF–Xα–SW (Table I) geometry-optimized, spin-unrestricted, transition-state calculation for $Ag_2$*[16] which set the equilibrium distance of $Ag_2$ at 2.84 Å, reasonably close to the EH value of 2.7 Å. Not unexpectedly, the Xα scheme exhibited a larger energy spread of the d-orbital manifold, a tendency which has been noted previously.[6] The correspondence between the calculated EH bond dissociation energy of 46 kcal/mol for $Ag_2$, the Xα value of 36 kcal/mol,[16] and the experimental gas-phase mass spectroscopy[18] value of 38 kcal/mol is also noteworthy.

**Dichromium, $Cr_2$.** We have previously reported EHMO and Xα calculations for the $Cr_2$ molecule and critically compared the two sets of data.[6] For the two major absorptions of matrix-entrapped $Cr_2$, an $s\sigma_g \rightarrow s\sigma_u$ and $d\pi_u \rightarrow p\sigma_g$ assignment seemed reasonable.[6] Furthermore, for a closed-shell, 12-electron system like $Cr_2$, the concept of a formally "sextuple" metal–metal bond was entertained in terms of two σ-, two π-, and two δ-orbital components. It was clear from these calculations that 3d–3d orbital overlap contributed to the main 4sσ–4sσ chromium–chromium bonding interaction. The bond dissociation energy was calculated to be 37 kcal/mol (at the equilibrium bond length of 1.7 Å), in line with the gas-phase mass spectroscopic value of 36.1 ± 6.9 kcal/mol determined for $Cr_2$.[18]

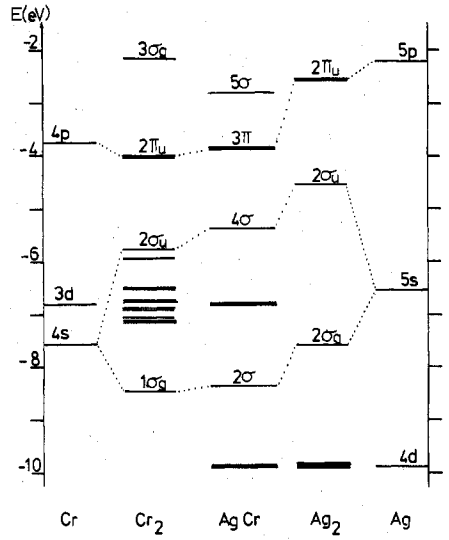


**Figure 7.** Extended Hückel molecular orbital energy level schemes calculated for $Ag_2$, $Cr_2$, and AgCr at their minimum energy geometries of 2.7, 1.7, and 2.9 Å respectively (see Table IV).

**Silverchromium, AgCr.** One might expect that a molecule such as AgCr, with metal atom components of quite disparate sizes and electronic type, would display properties somewhat distinct from those of the parent homonuclear diatomic molecules. Straightforward transference of the optimized EHMO parameters derived for $Ag_2$ and $Cr_2$ to AgCr leads to the molecular orbital scheme shown in Figure 7 (*it is worth noting here that this picture closely resembles the ground-state, spin-restricted Xα description of AgCr*[19]). In essence, one finds that the 3d orbitals of Cr and 4d orbitals of Ag are noninteracting in AgCr. The Cr 4s and Ag 5s orbitals were found to be the main contributors to the silver–chromium bond. The minimum-energy geometry for AgCr was computed for both closed- and open-shell configurations at 2.9 Å, considerably elongated with respect to the multiply bonded $Cr_2$ and slightly longer than the singly bonded $Ag_2$.

From the EHMO energy-level scheme for AgCr, three absorption bands can be expected within the 200–700-nm range of our instrument, $2\sigma \rightarrow 4\sigma$, $3\pi$, $5\sigma$ (Figure 7). The $2\sigma \rightarrow 4\sigma$ transition is calculated around 415 nm, in a region of overlap of atomic, diatomic, and triatomic features. The $2\sigma \rightarrow 3\pi$ transition is expected around 276 nm; we observe a AgCr absorption at 283 nm. The $2\sigma \rightarrow 5\sigma$ transition calculated at 224 nm might possibly be associated with the weak AgCr absorption at 220 nm (Table III).

**Table III.** Electronic Transitions of Major Significance in the $Cr_nAg_m$ Small-Cluster System[a]

| | | absn, nm | | | | absn, nm | |
|---|---|---|---|---|---|---|---|
| molecule | assignt[e] | calcd (EHMO) | obsd (Ar, 12–15 K) | molecule | assignt[e] | calcd (EHMO) | obsd (Ar, 12–15 K) |
| $Ag_2$ | $s\sigma_g \rightarrow s\sigma_u$ | 415 | 388/406 | $Cr_2$ | $s\sigma_g \rightarrow s\sigma_u$ | 460 | 460 |
| | $s\sigma_g \rightarrow p\pi_u$ | 251 | 258/262 | | $s\sigma_g \rightarrow p\pi_u$ | 280 | 263 |
| | $d\pi_g \rightarrow s\sigma_u$ | 233 | 227 | | | | |
| $Ag_3$ | $s\sigma_u \rightarrow s\sigma_g$ | 475 | 440 | $Cr_3$ | $s\sigma_u \rightarrow s\sigma_g$ | 500 | 477 |
| | $s\sigma_u \rightarrow p\pi_g$ | 345 | *b* | | $s\sigma_u \rightarrow p\pi_g$ | 467 | 477 |
| | $s\sigma_g \rightarrow p\pi_u$ | 234 | 245 | | $s\sigma_g \rightarrow p\pi_u$ | 251 | *d* |
| AgCr | $2\sigma \rightarrow 4\sigma$ | 415 | *c* | AgAgCr | $s\sigma \rightarrow p\pi$ | 269 | 276 |
| | $2\sigma \rightarrow 3\pi$ | 275 | 283 | | | | |
| | $2\sigma \rightarrow 5\sigma$ | 224 | 220 | | | | |

[a] Bond distances of Ag–Ag = 2.7 Å and Cr–Cr = 1.7 Å were employed in the pure-cluster calculations and Ag–Ag = 2.8 Å, Ag–Cr = 3.0 Å, and Cr–Cr = 2.0 Å in the bimetallic cluster calculations. [b] Overlap region with atomic silver. [c] Overlap region with atomic chromium. [d] Overlap region with dichromium. [e] Tentative optical assignments. Although the EHMO results of the present $Ag_mCr_n$ study seem entirely reasonable, they must be considered to be highly qualitative in nature, and any attempted quantitative assignment of optical transition energies must be treated with caution.

Table IV. Optimized Parameters Used in the Extended Hückel Calculations of $Cr_nAg_m$ Clusters

| | orbital | orbital exponent | $H_{ii}$, eV |
|---|---|---|---|
| Ag | 4p | 4.678 | −69.03 |
| | 4d | 3.805 | −9.82 |
| | 5s | 1.606 | −6.52 |
| | 5p | 1.354 | −2.20 |
| Cr | 3p | 3.817 | −56.22 |
| | 3d | 3.253 | −6.80 |
| | 4s | 1.285 | −7.60 |
| | 4p | 1.200 | −3.75 |

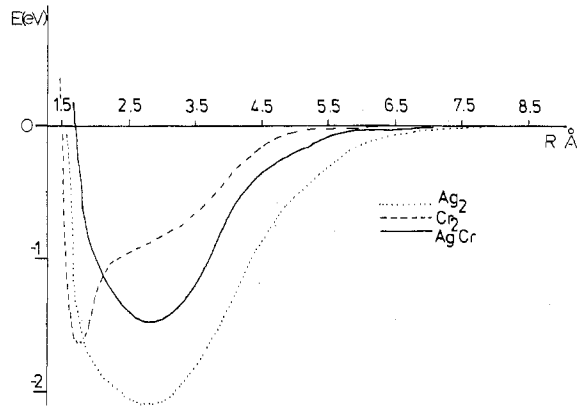


**Figure 8.** Potential energy curves calculated for $Ag_2$, $Cr_2$, and AgCr by using optimized EHMO parameters (see Table IV).

The bond dissociation energy of AgCr was calculated at the minimum-energy geometry to be 34 kcal/mol, which is slightly less than the values obtained for either $Ag_2$ or $Cr_2$, a not unexpected result for a 5s–4s bonded heteronuclear AgCr, when the $Ag_2$ and $Cr_2$ parent homonuclears involve the more favorable 5s–5s and 4s–4s/3d–3d orbital contributions, respectively (Figure 8 and Table IV).

## Extended Hückel Molecular Orbital Calculations on the Triatomic Molecules

Baetzold[12] has calculated the electronic and geometrical structures for several $Ag_n$ clusters comprising from 2 to 30 atoms by using EHMO and CNDO techniques and proposes a linear configuration to be most stable. Using a modified EH method, Anderson has proposed linear geometries for $Ni_3$ and $Cu_3$.[13] The effective-potential GVB–CI method of Goddard also favors a linear configuration for $Ni_3$.[24] Aside from $C_3$,[20] there really exists no definitive experimental precedent for favoring the linear geometry as the most stable form of three-atom metal clusters (see for example the recent ESR study of matrix-entrapped $Na_3$[21] and purported Raman spectrum of matrix-isolated $Ag_3$,[22a] which has since been shown to be a higher $Ag_n$ cluster unknowingly generated by 4880-Å laser photoaggregation[22b]).

In this study we have applied the optimized EH parameters for $Cr_2$ and $Ag_2$ to the various combinations of trinuclear, linear silver–chromium species and attempted to correlate the calculations with the available experimental data. In order to account for the probable bond elongations in passing from the diatomic to the triatomic species, we have performed geometry optimizations for some of the triatomic species. The Ag–Ag and Ag–Cr bond lengths were extended by 0.1 Å and the multiply bonded Cr–Cr bonds by 0.3 Å.

**Trisilver, $Ag_3$.** The optical spectrum of $Ag_3$ in solid Ar clearly exhibits two major bands at 440 and 245 nm with evidence for weaker absorptions accompanying the high-energy band (235 nm in Ar, a doublet being more apparent in Kr, Xe, and $CH_4$ matrices[8,23]). The EHMO scheme based on the linear configuration of $Ag_3$ exhibits a scenario not unlike that of $Ag_2$ in that the low-lying 4d Ag atomic orbitals remain essentially unperturbed in $Ag_3$ and are not involved in the silver–silver bonding (Figure 9). The 5s Ag atomic orbitals comprise most of the bonding in $Ag_3$, combining to form a filled $\sigma_g$-bonding, a half-filled, mainly nonbonding $\sigma_u$, and an empty $\sigma_g$-antibonding set of molecular levels. The high-lying virtual levels comprise the p band and are composed of similar linear combinations of $p\sigma$ and $p\pi$ Ag atomic orbitals. The potential energy minimum is again found at 2.7 Å.

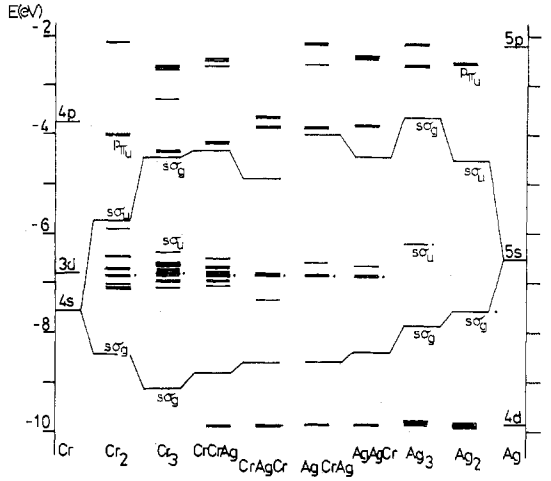


**Figure 9.** Extended Hückel molecular orbital energy level schemes calculated for the pure and mixed linear triatomic $Ag_mCr_n$ molecules at bond distances of Ag–Ag = 2.8 Å, Ag–Cr = 3.0 Å, and Cr–Cr = 2.0 Å for the mixed species (see Table IV). The Fermi level is indicated by a dot; lines connect the respective bonding and antibonding $\sigma$ orbitals.

Because of the qualitative nature and limitations of EHMO theory (indicated earlier) for calculating transition energies, it is clear that an unequivocal assignment of the electronic spectrum of $Ag_3$ is not possible. However, it seems likely that the intense, low-energy, 440-nm visible absorption of $Ag_3$ is associated with the HOMO–LUMO $(\sigma_g)^2(\sigma_u)^1(\sigma_g)^0 \rightarrow (\sigma_g)^2(\sigma_u)^0(\sigma_g)^1$ excitation, in line with recent SCF–X$\alpha$–SW calculations for linear $Ag_3$.[19] Assignment of the UV region of $Ag_3$ is much more contentious, although by analogy with $Ag_2$ one expects to observe $s\sigma \rightarrow p\sigma$, $p\pi$ optical excitations in the 230–250-nm region of the spectrum. Other excitations in the UV region are likely to involve transitions from the d band into the s band of $Ag_3$. A forthcoming SCF–X$\alpha$–SW study of small $Ag_n$ clusters ($n$ = 2–6) will examine this problem in detail.[19]

**Trichromium, $Cr_3$.** Our EHMO calculations for several $Cr_3$ geometries show a very slight preference for the linear configuration, with a minimum-energy geometry computed at 1.7 Å. As in $Cr_2$, the 3d orbitals contribute to the 4s chromium–chromium bonding in $Cr_3$, with the $\sigma$-bonding/$\sigma$-antibonding levels straddling the d band of $Cr_3$ as shown in Figure 9. A low-energy transition is expected around 500 nm which might be associated with the absorption observed at 477 nm. The reason for the uncertainty in geometry between linear, nonlinear, and triangular forms probably relates to the underestimation of the d-orbital splitting and d-orbital contribution to the metal–metal bonding in $Cr_3$. Because of the mixing of 4s/3d orbitals in $Cr_3$ and the intervention of the 3d band between the main 4s $\sigma$-bonding levels, optical assignments for $Cr_3$ are even more tenuous than for $Ag_3$, and spectral discussions will have to await the results of X$\alpha$ or ab initio molecular orbital calculations, as will the solution to the problem of a metastable $Cr_3$ species.[7]

**Disilverchromium, $Ag_2Cr$, and Silverdichromium, $AgCr_2$.** In the chromium–molybdenum system[7] it was possible to obtain

some useful optical data for $Cr_2Mo$ and $CrMo_2$ by photoselective-aggregation techniques. However, the band-overlap problem in the silver–chromium system is more serious in that only one band at 276 nm can be associated with a mixed trimer of, most probably, $Ag_2Cr$ composition. The EHMO calculations do not provide any further clues to solving the puzzle either. Nevertheless, an examination of the EHMO picture that emerges for AgAgCr, AgCrAg, AgCrCr, and CrAgCr atomic arrangements is interesting with regard to the effect of introducing a "foreign" atom into a transition-metal cluster and clearly relates to bonding and structure in bimetallic clusters at an atomic level.[2f]

Consider first the chromium system in Figure 9. The $Cr_2$ $\sigma$ molecular orbital comprising $4s/3d_{z^2}$ overlap and constituting the metal–metal bond is further stabilized (about 0.5 eV) on addition of a third Cr atom. Addition of a silver atom terminally to $Cr_2$ leads to a noticeably smaller stabilization of the metal–metal $\sigma$-bonding level, but still greater than the corresponding levels of $Cr_2$, $Ag_2$, and $Ag_3$, indicative of a genuine bonding interaction in AgCrCr in a bimetallic sense. The extent of chromium 3d–3d overlap remains essentially the same in AgCrCr as in $Cr_3$, with little evidence for overlap between the silver 4d and the dichromium 3d orbitals. However, placement of the silver atom between the two chromium atoms as in CrAgCr effectively collapses the Cr 3d–3d interaction (Figure 9) and further destabilizes the metal–metal $\sigma$-bonding level. These subtle electronic alterations on passing from an AgCrCr to a CrAgCr atomic arrangement point to the likely sensitivity of bimetallic cluster chemisorptive and catalytic properties to the relative disposition of the atomic constituents within the microcluster (uniformity of coclustering, surface composition, etc.[2f]).

In the silver system, the situation appears to be somewhat different. Although addition of a third silver atom to $Ag_2$ stabilizes the bonding $\sigma$ orbital (Figure 9), addition of a terminal chromium atom to $Ag_2$ to form AgAgCr lowers this metal–metal $\sigma$-bonding level still further (about 0.5 eV), while introduction of the third chromium atom between two silver atoms in AgCrAg lowers it even more (Figure 9). These data tend to support the contention that these Ag/Cr bimetallic combinations involve real chemical bonding rather than weak van der Waals type forces. It is interesting to contemplate that the orbital pictures of CrCrAg/CrAgCr could be interpreted in terms of an AgCr molecule onto which a Cr atom is chemisorbed at either the Ag end, giving an AgCr picture, or at the Cr end, giving a $Cr_2$-like scheme. Similarly, AgCrAg/AgAgCr might be viewed as chemisorption of a Ag atom onto a AgCr moiety, for which both the Ag and Cr ends produce an orbital scheme resembling the parent AgCr. These ideas are not entirely unlike those of Sinfelt et al.,[5b] who have rationalized the electron microscopy and EXAFS data for highly dispersed, Cu/Ru, silica-supported, bimetallic clusters in terms of two-dimensional, raft-like clusters and three-dimensional, spherical clusters of Ru, onto which Cu atoms are chemisorbed, where the cluster surface composition will depend on the state of dispersion and atomic composition of the metallic constituents of the catalyst.

## Conclusion

Apart from the unequivocal demonstration of photoselective bimetallic aggregation in the Cr/Ag system (supporting our earlier similar claim in the Cr/Mo system[7]), probably the single most impressive discovery is the fact that "molecular bimetallic $Cr_nAg_m$ clusters" actually have an independent and real existence as demonstrated by the generation and identification of AgCr and $Ag_2Cr$ in solid argon.

In view of the fact that Cr/Ag mixtures constitute a bulk alloy system which is categorized as of the immiscible variety,[9a] our discovery of "few-atom $Cr_nAg_m$ bimetallic molecules" must be construed to provide evidence in favor of a direct interaction between Cr and Ag atoms for a Sinfelt-type, highly dispersed and supported, Cr/Ag, bimetallic cluster. The EHMO computations tend to support this interactive model for small $Cr_nAg_m$ clusters. Although we must concede that such a bimetallic cluster system has not actually been reported in the literature, closely related Fe/Ag, Co/Ag, and Ni/Ag immiscibles have been purported to form bimetallic clusters in Sinfelt's patent publications.[1] We therefore feel relatively confident in proposing, on the basis of our very small $Cr_nAg_m$ cluster system, that the chemisorptive and catalytic results of Sinfelt[1,2a,2f,5a] and the Mössbauer spectroscopic investigations of Boudart, Garten, Ollis, and others[3a-3d] for "highly-dispersed" bimetallic cluster combinations comprising immiscible or low-miscibility metallic components are indeed likely to be reflecting a genuine and direct electronic (bonding) interaction between the different metal atoms, rather than a simple additive combination of the separate metal clusters. Moreover, we believe that our experimental failure, so far, to generate small, heteronuclear $Pd_mAg_n$ and $Pd_mMo_n$ metal molecules from Pd/Ag and Pd/Mo bimetal atom matrix cocondensations[26] (miscible and immiscible components, respectively, in the bulk phase and apparently noninteracting at the few-atom level under cryochemical conditions) lends further credence to the interactive model.

Clearly, other metallic combinations need to be investigated as a function of cluster size in the few-atom-cluster regime to further test our proposal. We fully intend to undertake such a program of research with a general thrust toward an electronic, structural, and chemical characterization of small, bimetallic and trimetallic clusters by UV–visible absorption and emission, infrared, Raman, and ESR spectroscopy in combination with EHMO/SCF-X$\alpha$-SW molecular orbital techniques.

**Acknowledgment.** We gratefully acknowledge the financial assistance of the National Research Council of Canada's Operating, New Ideas, and Strategic Energy Programmes, the Atkinson Foundation, the Connaught Fund, Imperial Oil of Canada, Erindale College, and Lash Miller Chemical Laboratories for support of this research.

**Registry No.** $Ag_2$, 12187-06-3; AgCr, 70355-37-2; $Ag_2Cr$, 70355-36-1; $Ag_3$, 12595-26-5; $Cr_2$, 12184-82-6; $Cr_3$, 66458-41-1; Ag, 7440-22-4; Cr, 7440-47-3.

## References and Notes

(1) J. H. Sinfelt et al., U.S. Patent, 3 871 997, Mar (1975); 3 901 827, Aug (1975); 3 429 619, Dec (1975); 3 953 368, Apr (1976).
(2) (a) J. H. Sinfelt, *Acc. Chem. Res.*, **10**, 15 (1977), and references cited therein; (b) J. H. Sinfelt, *Annu. Rev. Mater. Sci.*, **2**, 641 (1972); *J. Catal.*, **29**, 308 (1973); (c) D. W. McKee, *Trans. Faraday Soc.*, **61**, 2273 (1965); (d) R. Bouwman and W. M. H. Sachtler, *J. Catal.*, **19**, 127 (1970); (e) R. J. Kokes and P. H. Emmett, *J. Am. Chem. Soc.*, **81**, 5032 (1959); (f) J. H. Sinfelt and J. A. Cusumano in "Advanced Materials in Catalysis", J. J. Burton and R. L. Garten, Eds., Academic Press, New York, 1977, p 1; J. J. Burton and R. L. Garten, *ibid.*, p 33, and references cited therein.
(3) (a) C. H. Bartholomew and M. Boudart, *J. Catal.*, **29**, 278 (1973); (b) R. L. Garten and D. F. Ollis, *ibid.*, **35**, 232 (1974); (c) R. L. Garten, *ibid.*, **43**, 18 (1976); (d) M. A. Vannice and R. L. Garten, *J. Mol. Catal.*, **1**, 201 (1975).
(4) F. W. Lytle, *Nat. Bur. Stand. (U.S.), Spec. Publ.*, **No. 475**, 34 (1975); F. W. Lytle, D. E. Sayers, and E. B. Moore, *Appl. Phys. Lett.*, **24**, 45 (1974); I. W. Bassi, F. W. Lytle, and G. Parravono, *J. Catal.*, **42**, 139 (1976).
(5) (a) J. H. Sinfelt, Y. L. Lam, J. A. Cusumano, and A. E. Barnett, *J. Catal.*, **42**, 227 (1976), and references cited therein; (b) E. B. Prestridge, G. H. Via, and J. H. Sinfelt, *ibid.*, **50**, 115 (1977).
(6) W. Klotzbücher, G. A. Ozin, J. G. Norman, Jr., and H. J. Kolari, *Inorg. Chem.*, **16**, 2871 (1977).
(7) W. Klotzbücher and G. A. Ozin, *J. Mol. Catal.*, **3**, 195 (1977); *J. Am. Chem. Soc.*, **100**, 2262 (1978).
(8) H. Huber and G. A. Ozin, *Inorg. Chem.*, **17**, 155 (1978); S. Mitchell and G. A. Ozin, *J. Am. Chem. Soc.*, **100**, 6776 (1978).
(9) (a) M. Hansen, "Constitution of Binary Alloys", McGraw Hill, New York, 1958. (b) Subsequent studies employing Mg/M (where M = Cu, Ag, Au) codepositions with ESR detection (P. Kasai and D. McLeod,

*J. Phys. Chem.*, **82**, 1554 (1978)) and Fe/M (where M = Co, Ni, Cu) depositions with Mössbauer monitoring (P. A. Montano, *J. Appl. Phys.*, **49**, 1561 (1978)) speak highly of the tremendous potential that the matrix-isolation technique offers for studying the embryonic stages of bimetallic-cluster formation.
(10) P. Kündig, M. Moskovits, and G. A. Ozin, *J. Mol. Struct.*, **14**, 137 (1972).
(11) M. Moskovits and G. A. Ozin, *J. Appl. Spectrosc.* (*Engl. Transl.*), **26**, 487 (1972).
(12) R. C. Baetzold, *J. Chem. Phys.*, **55**, 4355 (1971); *ibid.*, **55**, 4363 (1971).
(13) A. B. Anderson, *J. Chem. Phys.*, **68**, 1744 (1978), and references therein.
(14) W. Klotzbücher, Ph.D. Thesis, University of Toronto, 1979.
(15) E. Clementi and J. Roetti, *At. Data Nucl. Data Tables*, **14**, 445 (1974); E. Clementi and D. L. Raimondi, *J. Chem. Phys.*, **38**, 2686 (1963).
(16) G. A. Ozin, H. Huber, D. McIntosh, S. Mitchell, J. C. Norman, and L. Noodleman, *J. Am. Chem. Soc.*, in press; paper first presented at the 175th Meeting of the American Chemical Society, Anaheim, CA, Mar 1978.
(17) B. Rosen, "Spectroscopic Data Relating To Diatomic Molecules", Pergammon Press, Elmsford, NY, 1970; J. Ruamps, *Ann. Phys.* (*Paris*), **13**(6), 1111 (1959), and references therein; C. M. Brown and M. L. Ginter, *J. Mol. Spectrosc.*, **69**, 25 (1978).
(18) K. H. Gingerich, *J. Cryst. Growth*, **9**, 31 (1971); J. Drowart in "Phase Stability in Metals and Alloys", Batelle Institute, 1966, p 305, and references cited therein.
(19) D. McIntosh, R. P. Messmer, and G. A. Ozin, to be submitted for publication.
(20) A. E. Douglas, *Astrophys. J.*, **114**, 466 (1951).
(21) D. M. Lindsay, D. P. Herschbach, and A. L. Kwiram, *Mol. Phys.*, **32**, 1199 (1976).
(22) (a) W. Schulze, H. U. Becker, R. Minkwitz, and K. Manzel, *Chem. Phys. Lett.*, **55**, 59 (1978); (b) W. Schulze, private communication.
(23) S. Mitchell, H. Huber, and G. A. Ozin, to be submitted for publication.
(24) W. A. Goddard, III, and T. Upton, private communication.
(25) R. C. Baetzold and R. E. Mack, *J. Chem. Phys.*, **62**, 1513 (1975); R. C. Baetzold, *Adv. Catal.*, **25**, 1 (1976).
(26) G. A. Ozin and W. Klotzbücher, "Photoselective Bimetallic Aggregation" in "Proceedings of the N.B.S. Materials Science Symposium", Washington, DC, 1978.

Contribution from the Department of Chemistry, Cornell University, Ithaca, New York 14853

# Perturbation Approach to Spin-Coupling Constants in the Phosphorus(III) Compounds

EVGENY SHUSTOROVICH*

*Received February 13, 1979*

The perturbation extension of the Pople–Santry theory developed earlier for treating the Fermi contact terms in reduced spin-coupling constants $^1K$(E–L) in substituted compounds $EL_{m-k}L'_k$ has been applied to main group "quasi lone pair" molecules, particularly to trigonal-pyramidal $P^{III}L_{3-k}L'_k$ ones. The three most important cases have been considered in detail, namely, for L = H, $P^{III}$, and F. The results obtained agree with experiment and explain the puzzling peculiarities of the observable $^1K(P^{III}–L)$ trends. The developed model permits both similarities and differences in the $^1K$(A–L) regularities for the A(HOS) vs. A(NHOS) compounds (highest vs. not highest oxidation states, respectively) to be explained and predicted.

## Introduction

Recently[1,2] we have developed the perturbation extension of the Pople–Santry (P–S) theory[3] for treating the Fermi contact (FC) terms in reduced nuclear spin coupling constants $^1K$(E–L) in substituted compounds $EL_{m-k}L'_k$ where E is a transition-metal M or main-group element A. We have found that for "one-pronged" ligands L with valence *ns* orbitals[2] such as H or $CR_3$ changes in $^1K$(E–L) under substitution should typically follow changes in the s contribution to the E–L bond overlap population.[1] On the other hand, for "two-pronged" ligands L, such as F, with a low lying lone $ns^2$ pair,[2] changes in $^1K$(E–F) in $EF_{m-k}L'_k$ are of rather complicated character depending on E, L′, and even *k*.[2]

The P–S theory for the FC term in $^1K$(E–L) was originally developed in explicit form for the $AL_4$ $T_d$ case.[3] One can show[2] that the simple and elegant P–S expression for the FC term holds for any compound $EL_m$ where, first, *all* ligands L are geometrically equivalent and, second, only *one* central atom orbital, $s_E$, belongs to the totally symmetric irreducible representation $A_1$. The linear $AL_2$,[1] planar-trigonal $AL_3$,[1,2] tetrahedral $AL_4$,[1,2] square $EL_4$,[1] and octahedral $EL_6$[1,2] compounds are just such cases. It is another story, however, for octet angular $AL_2$ and trigonal-pyramidal $AL_3$ compounds where only the first condition is valid but not the second as *two* central atom orbitals, $s_A$ and $p_z$, belong to the $A_1$ representation (see Table I). We can anticipate some peculiarities in the FC mechanism and therefore in trends of $^1K$(A–L) as compared, for instance, with those in linear $AL_2$ and trigonal-planar $AL_3$ compounds where A is of the highest oxidation state, A(HOS). We have recently developed a perturbation approach for treating the electronic structures and the substituent effects on the A–L bond lengths (strengths) in octet $AL_2$ and $AL_3$ molecules where A is not of the highest oxidation state, A(NHOS), and has quasi lone pairs (QLP).[4] In the present paper we will apply our perturbation approach to the substituent effects on spin-coupling constants $^1K$(A–L) in the mentioned QLP compounds.

* Address all correspondence to the author at: Chemistry Division, Research Laboratories, Eastman Kodak Co., Rochester, N.Y. 14650.

## Results and Discussion

The general LCAO MO form of the FC term is[3]

$$^1K(\text{A–L}) = C\cdot\sum_{i}^{\text{occ}}\sum_{j}^{\text{unocc}} (\epsilon_i - \epsilon_j)^{-1} c_{i\text{A}} c_{i\text{L}} c_{j\text{A}} c_{j\text{L}} \qquad (1)$$

where $C$ is some positive constant and the LCAO MO coefficients $c_{i\text{A}}$, $c_{j\text{L}}$, etc. correspond to the s parts of the occupied $\psi_i$ and unoccupied $\psi_j$ MO's with the energy gaps $E_{ij} = \epsilon_j - \epsilon_i > 0$. The valence $A_1$ MO's contributing to $^1K$(A–L) in octet $AL_2$ and $AL_3$ molecules (see Table I) have the following nodal structures[4]

$$\psi_3(3a_1) = s + p_z - \sigma^{(+)} \qquad (2)$$

$$\psi_2(2a_1) = -s + p_z + \sigma^{(+)} \qquad (3)$$

$$\psi_1(1a_1) = s + p_z + \sigma^{(+)} \qquad (4)$$

where the nodeless $\psi_1$ and one-node $\psi_2$ are occupied but the two-node $\psi_3$ is vacant. It is of great importance that in *all* octet $AL_2$ and $AL_3$ molecules the $\psi_2(2a_1)$ has the same nodal structure (3) corresponding to the p bonding but s antibonding.[4] The immediate consequence from eq 3 and 4 is a well-known fact that the A(NHOS)–L bonds are usually of less s character than the A(HOS)–L bonds[4] (cf. eq 10 and 11). The same nodal structures (2)–(4) remain in our approximate

0020-1669/79/1318-2108$01.00/0 